

Optically triggered Q-switched photonic crystal laser

Brett Maune, Jeremy Witzens, Thomas Baehr-Jones, Michael Kolodrubetz, Harry Atwater, and Axel Scherer

Department of Electrical Engineering and Applied Physics, California Institute of Technology, Pasadena, CA 91125, USA

bmaune@caltech.edu

Rainer Hagen

Bayer AG, Central Research/Physics Department, D-51368 Leverkusen (Germany)

Yueming Qiu

In Situ Technology and Experiments Systems Section, Jet Propulsion Laboratory, California Institute of Technology, Pasadena, CA 91109 USA

Abstract: An optically triggered liquid crystal infiltrated Q-switched photonic crystal laser is demonstrated. A photonic crystal laser cavity was designed and fabricated to support two orthogonally polarized high-Q cavity modes after liquid crystal infiltration. By controlling the liquid crystal orientation via a layer of photoaddressable polymer and a writing laser, the photonic crystal lasing mode can be reversibly switched between the two modes which also switches the laser's emission polarization and wavelength. The creation of the Q-switched laser demonstrates the benefits of customizing photonic crystal cavities to maximally synergize with an infiltrated material and illustrates the potential of integrating semiconductor nanophotonics with optical materials.

©2005 Optical Society of America

OCIS codes: (230.3720) Liquid-crystal devices; (140.5960) Semiconductor lasers

References and Links

1. E. Yablonovitch, "Inhibited spontaneous emission in solid-state physics and electronics," *Phys. Rev. Lett.* **58**, 2059-2062, (1987).
2. S. John, "Strong localization of photons in certain disordered dielectric superlattices," *Phys. Rev. Lett.* **58**, 2486-2489, (1987).
3. Y. Akahane, T. Asano, B. Song, and S. Noda, "High-Q photonic nanocavity in a two-dimensional photonic crystal," *Nature* **425**, 944-947, (2003).
4. S. Noda, A. Chutinan, and M. Imada, "Trapping and emission of photons by a single defect in a photonic bandgap structure," *Nature* **407**, 608-610, (2000).
5. O. Painter, R. K. Lee, A. Scherer, A. Yariv, J. D. O'Brien, P. D. Dapkus, and I. Kim, "Two-dimensional photonic band-gap defect mode laser," *Science*, **284**, 1819-1821, (1999).
6. J. Vuckovic, M. Loncar, H. Mabuchi, and A. Scherer, "Design of photonic crystal microcavities for cavity QED," *Phys. Rev. E* **65**, 016608-1-11, (2002).
7. B. Lev, K. Srinivasan, P. Barclay, O. Painter, and H. Mabuchi, "Feasibility of detecting single atoms using photonic bandgap cavities," *Nanotechnology* **15**, S556-S561, (2004).
8. M. Fujita, S. Takahashi, Y. Tanaka, T. Asano, and S. Noda, "Simultaneous inhibition and redistribution of spontaneous light emission in photonic crystals," *Science* **308**, 1296-1298, (2005).
9. T. Yoshie, A. Scherer, J. Hendrickson, G. Khitrova, H. M. Gibbs, G. Rupper, C. Ell, O. B. Shchekin, and D. G. Deppe, "Vacuum Rabi splitting with a single quantum dot in a photonic crystal nanocavity," *Nature* **432**, 200-203, (2004).
10. A. Badolato, K. Hennessy, M. Atature, J. Dreiser, E. Hu, P. Petroff, and A. Imamoglu, "Deterministic coupling of single quantum dots to single nanocavity modes," *Science* **308**, 1158-1161, (2005).
11. K. Busch, and S. John, "Liquid-crystal photonic-band-gap materials: the tunable electromagnetic vacuum," *Phys. Rev. Lett.* **83**, 967-970, (1999).
12. E. Yablonovitch, "Liquid versus photonic crystals," *Nature* **401**, 539-541, (1999).

13. S. W. Leonard, J. P. Mondia, H. M. van Driel, O. Toader, S. John, K. Busch, A. Birner, U. Gosele, and V. Lehmann, "Tunable two-dimensional photonic crystals using liquid-crystal infiltration," *Phys. Rev. B* **61**, R2389-R2392, (2000).
14. C. Schuller, F. Klopff, J. P. Reithmaier, M. Kamp, and A. Forchel, "Tunable photonic crystals fabricated in III-V semiconductor slab waveguides using infiltrated liquid crystals," *Appl. Phys. Lett.* **82**, 2767-2769, (2003).
15. D. Kang, J. E. MacLennan, N. A. Clark, A. A. Zakhidov, and R. H. Baughman, "Electro-optic behavior of liquid-crystal-filled silica opal photonic crystals: effect of liquid-crystal alignment," *Phys. Rev. Lett.* **86**, 4052-4055, (2001).
16. Y. Shimoda, M. Ozaki, and K. Yoshino, "Electric field tuning of a stop band in a reflection spectrum of synthetic opal infiltrated with nematic liquid crystal," *Appl. Phys. Lett.* **79**, 3627-3629, (2001).
17. R. Ozaki, T. Matsui, M. Ozaki, and K. Yoshino, "Electrically color-tunable defect mode lasing in one-dimensional photonic-band-gap system containing liquid crystal," *Appl. Phys. Lett.* **82**, 3593-3595, (2003).
18. R. Hagen, and T. Bieringer, "Photoaddressable polymers for optical data storage," *Adv. Mater.* **13**, 1805-1810, (2001).
19. M. Loncar, A. Scherer, and Y. Qiu, "Photonic crystal laser sources for chemical detection," *Appl. Phys. Lett.* **82**, 4648-4650, (2003).
20. B. Maune, M. Loncar, J. Witzens, M. Hochberg, T. Baehr-Jones, D. Psaltis, A. Scherer, and Y. Qiu, "Liquid-crystal electric tuning of a photonic crystal laser," *Appl. Phys. Lett.* **85**, 360-362, (2004).
21. J. T. Ho, J. T. "Light scattering and quasielastic spectroscopy," in *Liquid Crystals*, S. Kumar, ed. (Cambridge University Press, Cambridge UK, 2001), pp. 197-239.
22. By infiltrating the lasers with refractive index calibrated fluids and comparing the lasing redshift with that of the LC infiltrated lasers, we estimated the IR refractive indices of the LC to be $n_o = 1.47$ and $n_e = 1.58$. This analysis assumed the LC spontaneously arranged itself randomly within the PC.
23. S. Lucht, D. Neher, T. Miteva, G. Nelles, A. Yasuda, R. Hagen, and S. Kostromine, "Photoaddressable polymers for liquid crystal alignment," *Liq. Cryst.* **30**, 337-344, (2003).
24. K. Srinivasan, P. Barclay, O. Painter, J. Chen, A. Cho, and C. Gmachl, "Experimental demonstration of a high-quality factor photonic crystal microcavity," *Appl. Phys. Lett.* **83**, 1915-1917, (2003).
25. The simulated cavity Qs are for PCs with an isotropic ambient refractive index. Simulations involving anisotropic ambient refractive indices that mimic the infiltrated LC (in particular asymmetric cladding/hole layer configurations) yield lower Qs [26].
26. C. Kim, W. Kim, A. Stapleton, J. Cao, J. O'Brien, P. Dapkus, "Quality factors in single-defect photonic-crystal lasers with asymmetric cladding layers," *J. Opt. Soc. Am. B* **19**, 1777-1781, (2002).
27. M. Loncar, T. Yoshie, A. Scherer, P. Gogna, and Y. Qiu, "Low-threshold photonic crystal laser," *Appl. Phys. Lett.* **81**, 2680-2682, (2002).
28. G. S. Hartley, "The cis-form of azobenzene," *Nature* **140**, 281 (1937).
29. B. Lachut, S. Maier, H. Atwater, M. Dood, A. Polman, R. Hagen, and S. Kostromine, "Large spectral birefringence in photoaddressable polymer films," *Adv. Mater.* **16**, 1746-1750, (2004).
30. V. Cimrová, D. Neher, S. Kostromine, and T. Bieringer, "Optical anisotropy in films of photoaddressable polymers," *Macromolecules* **32**, 8496-8503, (1999).
31. Y. Saba, M. Yamamoto, H. Watanabe, T. Bieringer, D. Haarer, R. Hagen, S. Kostromine, and H. Berneth, "Photoaddressable polymers for rewritable optical disk systems," *Jpn. J. Appl. Phys.* **40**, 1613-1618, (2001).
32. M. Eich and J. H. Wendorff, "Erasable holograms in polymeric liquid crystals," *Makromol. Chem., Rapid Commun.* **8**, 467-471, (1987).

1. Introduction

Interest in photonic crystal (PC) [1,2] cavities has steadily grown in recent years as researchers continue to discover new applications for their unique ability to strongly confine light in volumes approaching a cubic wavelength. These structures are suitable for high-quality-factor (high-Q) nanocavities [3], optical filters [4], compact lasers [5], cavity quantum electrodynamics [6-8], and quantum information processing [9,10], amongst others. As promising and as diverse as these applications are, they are based on "traditional" (air-filled) PC cavities. A relatively unexplored but important aspect of PC cavities is that their intrinsic porous structure enables efficient integration with fluids [11,12] and polymer featuring a wide array of optical properties. Integrating PC cavities with these materials can take full advantage of the tremendous design freedom and unique optical properties inherent in the cavities. In this letter, we report on the use of birefringent liquid crystal (LC) [13-17] and photoaddressable polymer (PAP) [18] to create optically triggered Q-switched PC lasers. The Q-switched laser represents an initial example of an electromagnetically optimized opto-fluidic device which capitalizes on the synergy between PC cavities and birefringent

materials. Further customization of PC cavities tailored to the unique properties of an infiltrated material will enable novel applications and lead to new directions in PC research.

Microfabricated PC lasers enable the efficient interaction of the confined lasing field with infiltrated materials. Although the light emitting into the lasing mode is generated within the semiconductor material, it is possible to design high-Q optical cavities in which a large fraction of the mode's electromagnetic energy is concentrated within the PC's holes and cladding layers. This property of PC lasers enables the introduction of materials featuring a wide variety of optical properties through infiltration into the holes of the PC or by depositing the materials to form the cladding layers. Previously it has been shown that the PC laser wavelength can be tuned by back-filling the PC with various liquids [19] or by controlling the orientation of infiltrated nematic LC with electrostatic fields [20]. Such tuning methods rely upon changing the cavity's effective refractive index and the optical path length corresponding to a *single* lasing mode. Here we demonstrate a fundamentally different approach to tuning PC lasers based on switching the lasing mode between one of *two* high-Q modes supported by the cavity. Whereas traditional Q-switching yields pulsed lasing from temporally modulating a single cavity mode's Q, the Q-switching presented here involves selecting the lasing mode by quasi-statically modulating the relative Qs of two cavity modes. This method utilizes a carefully designed PC cavity which features a modal structure to optimally interact with birefringent materials. The Q-switching significantly enhances the wavelength emission range of PC lasers by largely decoupling the tuning with the infiltrated material's birefringence and simultaneously enables control over the lasers' emission polarization. The Q-switched PC laser demonstrates the enormous potential of PC-based nanophotonics and suggests even higher levels of optical functionality can be achieved.

2. Liquid crystal considerations and cavity design

Although infiltration of PC cavities with LCs enables spectral tuning, the cavity's Q substantially decreases due to the higher refractive index of the LC. The lower Q arises from a smaller refractive index contrast between the PC slab and LC cladding layers, reducing vertical confinement of the optical mode. Moreover, light scattering from heterogeneously oriented or misaligned LC molecules results in further laser losses [21]. Thus, infiltration of a PC cavity with LC presents a tradeoff between decreasing Qs and increases in cavity tunability. Consequently, the nematic LC chosen for this project (ZLI-3086 from Merck) offers a compromise which features adequate birefringence for tunability ($n_o = 1.5040$, $n_e = 1.6171$ at 589 nm) [22] while simultaneously exhibiting a reasonably low n_o and n_e values to obtain sufficient cavity Qs for lasing. A further benefit of LC ZLI-3086 is its ability to be aligned by PAP, rendering it optically controllable and avoiding the need for electrostatic contacts [23].

The Q-switched PC laser is based on a cavity design that supports two orthogonally polarized modes with high Qs—even after LC infiltration. Extensive finite-difference time-domain (FDTD) simulations were conducted to develop a cavity geometry that maximized the Qs of both modes with an ambient refractive index of 1.5. Incidentally, optimizing a family of cavity designs immersed in air (ambient refractive 1.0) usually does not correspond to the optimal design for an ambient refractive index of 1.5. A scanning electron microscope image of the optimized cavity is shown in Fig. 1. The cavity combines a square-like lattice defect embedded within a graded hexagonal lattice [24]. This cavity geometry yields two dipole-like high-Q modes, one polarized along the X axis of the crystal and the other polarized along the Y axis (Fig. 2(a) and (b)). Simulations of Q values as a function of ambient refractive index are summarized in Fig. 2(c). The X and Y modes feature a Q of approximately 12,000 and 30,000, respectively in air and remain above 4,000 even when the PC is surrounded by an ambient refractive index of $n \sim 1.5$. Photonic crystal lasers using this design were constructed from InGaAsP quantum well material by using a combination of electron beam lithography and dry etching. Details of the laser fabrication procedure have been described elsewhere [26]. After fabrication, the lasers were infiltrated with the LC, and cells were constructed around the lasers which included a PAP alignment layer (Fig. 3(a)) (see Appendix). Finally, the

tunable PC lasers were mounted in an optical test setup (shown in Fig. 3(b)) for characterization.

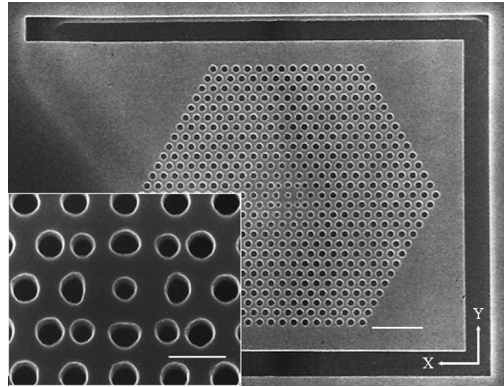


Fig. 1. Scanning electron micrograph of a fabricated 2D PC laser. The periodicity of holes is 450 nm. The inset shows a close up of the cavity geometry taken with a sample tilted 15°. Scale bar, 2 μm . Inset scale bar, 1 μm .

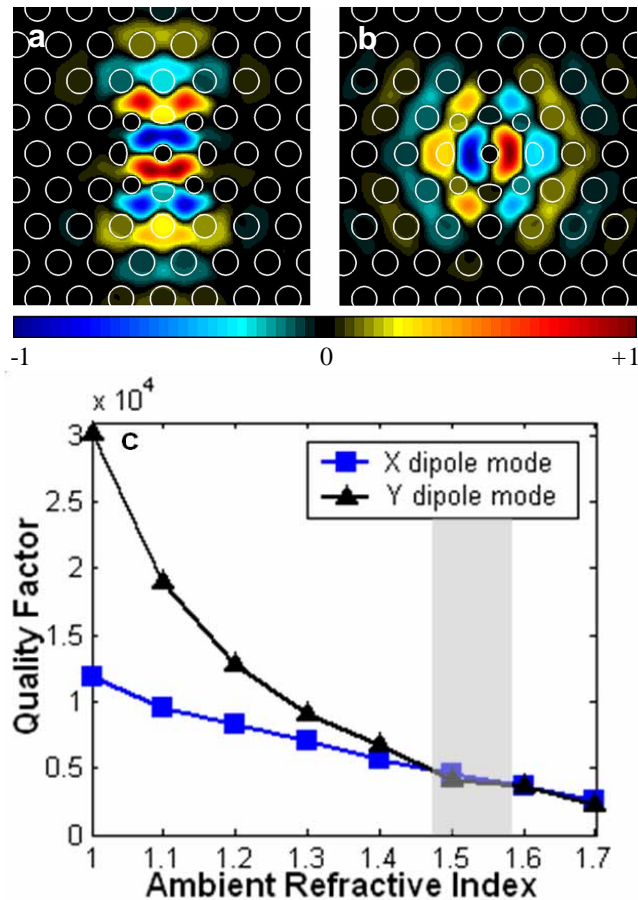


Fig. 2. Photonic crystal cavity modes and simulated Qs. Finite-difference time-domain simulation of Z component of magnetic field for **a**, X-polarized and **b**, Y-polarized modes. **c**, Simulated Q for X and Y-polarized cavity modes as a function of the ambient refractive index. Although the X-polarized mode has a Q significantly below that of the Y-polarized mode in air, both possess comparable Qs above 4000 even at an ambient refractive index of $n \sim 1.5$ [25]. Shaded region denotes ambient refractive index accessible by the infiltrated LC [22].

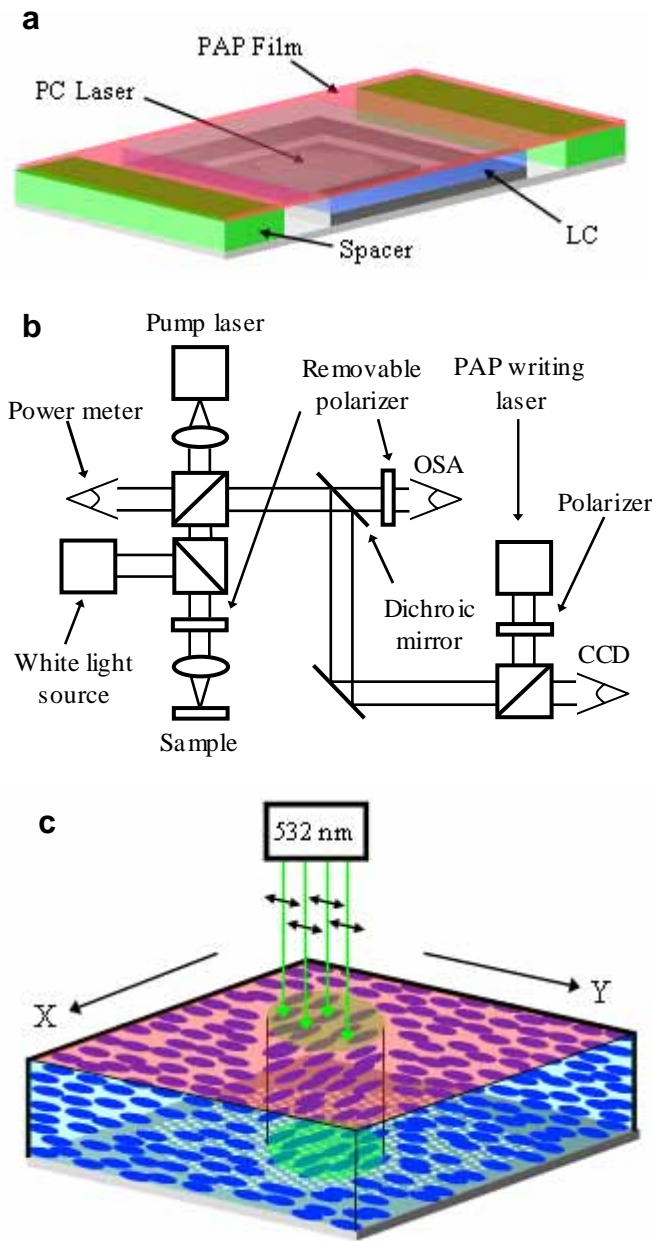


Fig. 3. Schematics of LC cell, optical setup, and PAP/LC photoinduced alignment. **a**, Schematic of PC laser LC/PAP cell. Thickness of LC and PAP films are approximately $5\ \mu\text{m}$, and $31 \pm 1\ \text{nm}$, respectively. Top coverslip is not shown. **b**, Schematic of PC laser optical characterization setup. **c**, Schematic representation of the LC reorientation via PAP photoinduced alignment. The PAP orients itself orthogonally (along X axis) with respect to the writing laser polarization direction (Y axis) which in turn induces a similar alignment in the LC.

3. Experimental realization of Q-switching

Lasing spectra were recorded by optical pumping of the PC cavities while systematically varying the LC orientation in the top cladding layer via the PAP layer. The PAP orientation is controlled by illuminating the PC laser with polarized 532 nm light from a frequency-doubled Nd:YAG laser (Fig. 3(b)). As the PAP orients itself orthogonally with respect to the writing laser polarization [18,28,29], the LC molecules are in turn oriented parallel to that layer [23] (Fig. 3(c)). Immediately after spin-coating, the PAP possessed a planar orientation [30] but invariably underwent photobleaching [31] as it was repeatedly written throughout the measurement process. A typical measurement cycle consists of first writing the PAP with the green laser and subsequently pumping the PC cavity with a near-IR laser. The laser spectrum can then be recorded with an optical spectrum analyzer (see Appendix).

Spectra recorded for a PC cavity that supports two high-Q lasing modes are shown in Fig 4 and 5. As the PAP's orientation is varied from the Y to the X axis, the LC in contact with the PAP undergoes the same rotation, and this realignment propagates through the bulk LC in the cladding layer above the laser cavity. Due the cavity modes' orthogonality, as the LC is rotated from the Y axis to the X axis one cavity mode experiences a maximum cladding index (n_c) whereas the other mode experiences a minimum in the refractive index (n_o). As the refractive index of one mode increases, its lasing wavelength red-shifts and its Q decreases until the lasing is quenched by increased losses and gain competition with the other mode. Conversely, the orthogonal mode's resonance blue-shifts and its Q increases until that mode is driven above threshold and starts lasing. Thus, rotating the LC switches the laser output from one polarized mode to the other. This switching between lasing cavity modes effectively amplifies the spectral emission range of the cavity far beyond what would be possible by tuning the cavity length of a single mode. The switching in the PC lasers is both reversible and reproducible as supported by many switching cycles with little loss in fidelity.

4. Discussion and conclusions

The tuning of each individual cavity resonance seen in Fig 5 (X-polarized ~1.4 nm, Y-polarized ~1.5 nm) is attributed to changes in the effective optical path lengths experienced by the cavity modes due to the rotated LC. Given the magnitude of the resonance shifts, FDTD computer simulations suggest only the LC in the top cladding layer follows the PAP orientation. The LC in the PC holes can experience relatively strong surface anchoring, which inhibits the cladding LC orientation from propagating into the PC holes [13,20]. One possibility for circumventing this limitation in the future is to eliminate the LC and instead infiltrate the PC with the PAP itself. The underlying alignment mechanism for PAP (photo-induced isomerization cycles) is fundamentally different than for LC and therefore PAP may be relatively immune to surface effects present within the confined geometries of PC holes. The ability to control the orientation of PAP, LC, or some other birefringent material in the holes of a PC would not only significantly increase optical-path-length-based tuning, but could also enable more complicated switching behavior in PC cavities supporting more modes by increasing the selectivity between the modes.

The wavelength switching range of the PC laser is not limited by the birefringence of an infiltrated material but ultimately may be limited by the quantum well gain spectra. Future enhancements in the quantum well structure and cavity design can potentially further increase the wavelength switching range far beyond the observed 7 nm. Lasing after LC infiltration requires maximal gain and minimal losses and both lasing modes are observed close to 1550 nm, the engineered maximum of the quantum well emission. If the grown quantum well structure were re-designed to exhibit two distinct maxima in the gain spectra and if the orthogonally polarized PC cavity modes can be designed to coincide with these gain maxima, then the laser emission may be switched over a wavelength range exceeding 100 nm.

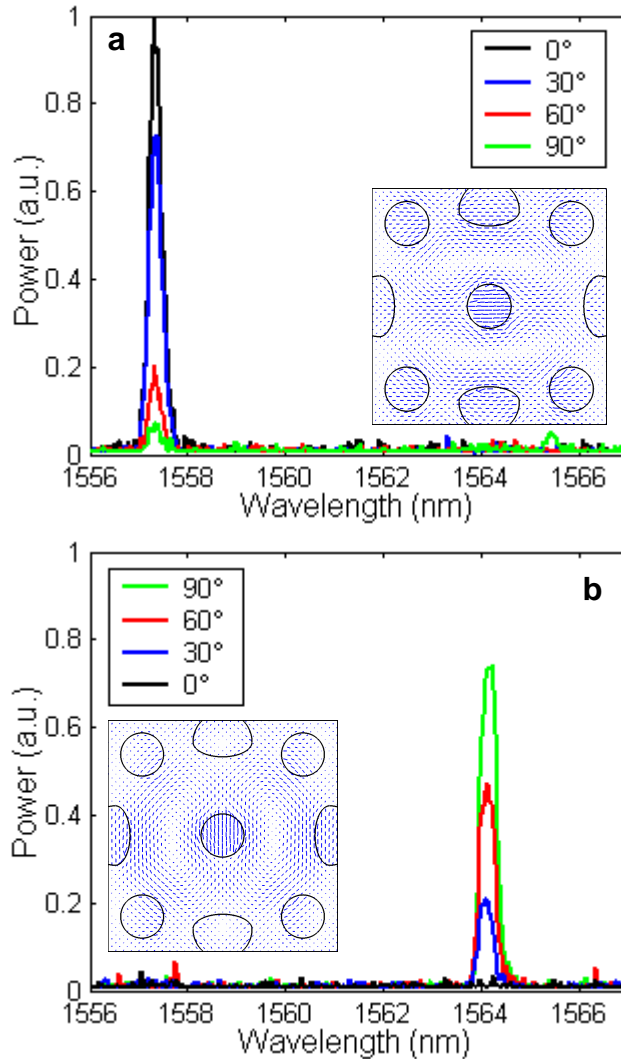


Fig. 4. Confirmation of orthogonally polarized lasing modes. **a**, The laser spectra is taken with PAP/LC aligned with the Y axis and the collected light is passed through a polarizer oriented at various angles. The collected power is maximized with the polarizer oriented at 0° (X axis) and minimized at 90° (Y axis) which indicates the resonance is the X-polarized dipole mode. **b**, The laser spectra is taken with the same conditions as in **a** but with the PAP/LC aligned with the X axis. The collected power is maximized with the polarizer oriented at 90° (Y axis) and minimized at 0° (X axis) which indicates the resonance is the Y-polarized dipole mode. Insets **a** and **b** show simulation of cavity modes' polarization profile. The spectra in parts **a** and **b** are normalized to the same power.

The integration of nanophotonics with birefringent nonlinear materials enables the complete utilization of polarization as a degree of freedom and may form the basis of future integrated opto-fluidic systems. In particular, the Q-switched PC lasers can potentially fulfill a variety of scientific and technological needs. The LC PC laser can serve as a polarization sensitive optically triggered switch within optical information processing architectures. Furthermore since the PAP orientation is stable, no external energy or input, such as an electrostatic field, is required for the laser to maintain its lasing wavelength and polarization. Liquid crystal PC laser arrays can also serve as an optical re-programmable read-only memory elements. More significantly, the successful integration of LC and PAP (itself a material with

enormous potential with photonics integration) [18,31,32] in the creation of the Q-switched PC laser illuminates the extraordinary design freedom and capabilities of PC cavities and further demonstrates the full potential of integrating semiconductor nanophotonics with nonlinear optical fluids and polymers.

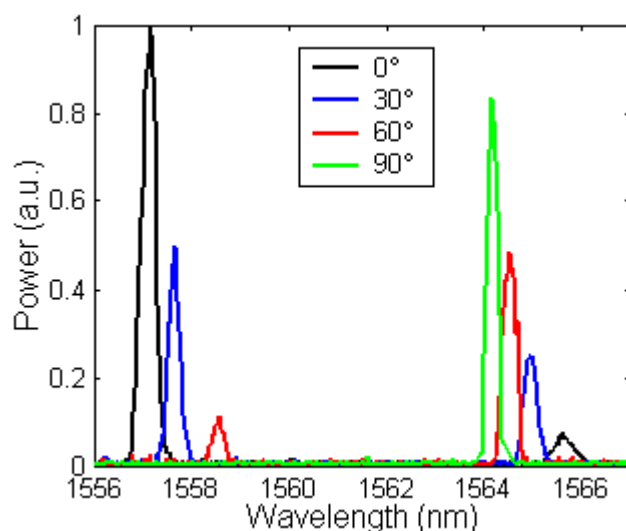


Fig. 5. Experimental realization of Q-switching. The laser spectra is taken after PAP writing laser aligns the PAP/LC at several orientations. After writing at 0° (PAP writing laser polarized along X axis which causes PAP/LC to orient along Y axis), emission is maximized for the X-polarized mode and minimized for the Y-polarized mode. As the PAP writing laser polarization is rotated towards 90° , the cladding refractive index for the X mode increases, raising losses until the lasing is quenched and emission terminates. Meanwhile, the Y mode experiences a decreasing refractive index, lowering cavity losses and driving the mode above threshold and lases.

Acknowledgments

The authors would like to thank Eric Kelsic, Beth Lachut, Robb Walters, Tomoyuki Yoshie, and Zhaoyu Zhang for valuable discussions. Funding for this work by DARPA as part of the Center for Optofluidic Integration is also gratefully acknowledged.

Appendix

PAP film fabrication

The PAP used in this study contains azobenzene chromophores and mesogenic side groups [29] and was dissolved in tetrahydrofuran with a concentration of 15 g/L. The solution was mixed for 10 minutes with a magnetic stir bar to help ensure complete dissolution of the PAP in the solvent. The PAP was then spun on a coverslip at 3500 RPM for 40 s. The PAP was deposited on the coverslip after the coverslip was already spinning at the target RPM to aid in creating a homogenous film. Finally, the PAP samples were baked on a hotplate at 60°C for 10 min to ensure complete solvent removal. Atomic force microscopy measurements indicate the PAP film thickness to be 31 ± 1 nm with an estimated surface roughness of 1 nm.

Liquid crystal cell fabrication

To construct the LC cell around the lasers, the sample along with two spacers were attached to a glass microscope slide with polymethylmethacrylate (PMMA). Next, a drop of the LC ZLI-3086 was placed on the PC sample and the PAP film/coverslip was glued to the spacers with

the PAP film facing towards the LC. The spacers were sufficiently thick to obtain an estimated 5 μm gap between the sample and PAP film.

Photoaddressable polymer writing

The PAP was written using 532 nm light from a frequency-doubled Nd:YAG laser with an intensity ranging from 6 W/cm^2 (x polarization) to 12 W/cm^2 (y polarization) and a spot size of approximately 11 μm . To ensure writing saturation, the PAP was written for intervals of one second, although the onset of tuning was observed even for the shortest writing intervals of approximately 10 ms. The PAP writing time can likely be reduced further to ~ 100 μs with little loss in writing efficiency. The PAP writing occurs during photo-induced isomerization cycles between the trans and cis conformations of the azo moiety and has an absorption cutoff of approximately 630 nm [29]. The visible absorption cutoff is critical for it means the pump beam (830 nm) does not write the PAP. A low intensity white light was necessary for imaging purposes to initially locate individual PC laser samples. A removable polarizer oriented along the Y axis was always used with the white light to prevent photobleaching and to initialize the PAP to the same orientation for the subsequent laser characterization.

Laser characterization

Lasing after LC infiltration was confirmed by the recording of a characteristic output power versus input power curve (L-L curve). The lasing modes were also linearly polarized in agreement with FDTD simulations (see Insets Fig. 4(a) and 4(b)). The PC lasers were pumped with 4.3 mW from a semiconductor laser diode at 830 nm with a pulse length of 30 ns and a periodicity of 3.0 μs . Pump light was transmitted through the transparent coverslip, PAP film, and the LC onto the PC slab.